

REVISITING TWO PHASE NMR DATA WITH A NEW INVERSION ROUTINE USING A TRIANGULAR PORES MODEL FOR WETTABILITY ESTIMATION

Unn Højgaard á Lað¹, Aksel Hiorth¹, Ola Ketil Siqveland² and Svein M. Skjæveland².
¹International Research Institute of Stavanger, ²University of Stavanger.

This paper was prepared for presentation at the International Symposium of the Society of Core Analysts held in Noordwijk, The Netherlands 27-30 September, 2009

ABSTRACT

NMR measurements are sensitive to the wettability because of the surface relaxivity of the pore surface that enhances the relaxation of the fluids inside the porous media. It has been shown in numerous publications that NMR can detect changes in wettability and many different approaches have been taken for finding the wettability by NMR. The NMR magnetic decay curve is commonly inverted to a T_2 distribution. The distribution is then used to estimate wettability changes based on shifts in the distribution or specific T_2 values such as the logarithmic mean of the T_2 distribution.

We have developed an inversion routine that fits the decay curve to a distribution of triangular pores. The triangular pores make it possible to model two immiscible fluids simultaneously present in the same pore. We get pore saturation and wettability as functions of pore size, contact angle and capillary pressure. The corresponding NMR signal is calculated based on a previously published correlation for the magnetic signal of two immiscible phases in triangular pore geometry. The resulting output from the inversion routine is a pore size distribution, saturation, separate oil and water distributions and a wettability index based on fluid-pore surface areas for the oil and water.

We have tested the inversion routine on previously published CPMG NMR measurements of Berea cores at 100 % water saturation, immediately after flooding with dead crude and after aging. Based on the calculated pore size distribution at 100 % saturation and after flooding, we estimate bulk relaxation and surface relaxivity for the water and oil. We use measured saturations to tune the inversion. The wettability index is compared to spontaneous water imbibition after aging. We find good agreement between wettability index and spontaneous imbibition measurements after aging.

We have investigated how the calculated fluid distributions, wettability index and T_2 distribution behave as functions of the NMR signal and the choice of model- and NMR-parameters. Comparing the regular T_2 distribution with the T_2 distribution from the new inversion we find that the new T_2 distribution has the same features, but the peaks are sharper and separate for oil and water. We find that using an inversion routine with a pore model is very informative for inferring the effects of the parameters. This can be useful when interpreting NMR data.

INTRODUCTION

When fluids inside the porous media come in contact with the pore surface, the surface relaxation of the surface enhances the magnetic decay. This effect has been used in previous work to connect change in wettability with change in the NMR signal. Borgia et al. [1] estimated wettability changes from obtained relaxation rates. Howard [2] compared relative T_1 to results obtained from Amott tests. Fleury and Deflandre [3] calculated a wettability index based on peak relaxation times at four different saturations that agreed well with the USBM index. Freedman et al. [4] introduced a new diffusion editing pulse sequence for distinguishing water signal from oil signal. Looyestijn and Hofman [5] used the T_2 distribution measured at 100 % water saturation as a pore size distribution. Based on a model for fluid distributions they calculated the NMR response at different saturations and by tuning the parameters governing the magnetic decay, they matched the experimental NMR response. When the match was found, the parameters gave a wettability index. The resulting wettability index compared well with the USBM index. The inclusion of pore network modelling is well founded and pore network modelling has been shown to reproduce the main characteristics of both water-wet and mixed-wet reservoirs. An example of a complex model is presented by Øren et al. [6]. The model is based on thin-section image analysis. From the model they simulated primary drainage and water injection and the results were in good agreement with the experimental data. Random Walk generated NMR responses were in fair agreement with experimental results. Simpler models have been proposed that are based on triangular pores. The triangular geometry allows for pores having several phases present simultaneously, Helland and Skjaeveland [7]. The same authors showed that it was possible to reproduce the main characteristics of mixed-wet capillary pressure curves using a bundle-of-triangular-tubes model, Helland and Skjaeveland [8]. Al-Mahrooqi et al. [9] used a bundle-of-triangular-pores model to estimate the T_2 distribution for two immiscible phases. The results were in good agreement with the obtained experimental results.

In this work we present a preliminary inversion routine, where the NMR data is fitted directly to a pore model of triangular pores for wettability determination. The inversion matrix \mathbf{K} is based on a correlation that we have developed, Lad et al. [10], where the magnetic signal for each pore is divided into a signal from the oil and the water. The signal from each fluid is in turn calculated using two relaxation times, which gave a better fit to Random Walk simulations than the standard mono-exponential function with only one relaxation time T_2 and was valid outside the Fast Diffusion Limit.

THEORY

Inversion routine

Nuclear Magnetic Resonance, NMR induces a short lived magnetization of a sample by aligning the spins of the molecules in the sample. The spins of the hydrogen molecules are then excited and tilted in a direction where their magnetization can be measured by a RF-pulse. The magnetization decays as the sample reverts back towards an equilibrium state. For interpretation the measured magnetic decay $m(t)$ is inverted to a distribution $f(T_2)$ of exponential functions decaying at distinct relaxation times T_2 and errors ε given by

$$m(t) = \int f(T_2) \exp\left(-\frac{t}{T_2}\right) dT_2 + \varepsilon(t). \quad (1)$$

This is known as a Fredholm integral of the first order. The solution of this kind of problem is known to be ill-conditioned and one of the issues with this kind of problem is the lack of uniqueness of inversion results. In theory there exist infinitely many solutions. One method of increasing the uniqueness is to impose a Tikhonov regularization on the inversion routine, Tikhonov and Arsenin [11] that improves the stability of the solution. This regularization dictates that the obtained distribution be smooth. Still the solution is not unique. An additional constraint for inverting NMR data requires that the distribution $f(T_2)$ is non-negative. Inversion with Tikhonov regularization is given by

$$\min_f \left(\|\mathbf{K}F - G\|^2 + \alpha \|F\|^2 \right), \quad (2)$$

where $\|\cdot\|$ denotes the Euclidian norm. \mathbf{K} is a $N \times M$ matrix, F is the distribution of the columns in \mathbf{K} and has the dimension $1 \times M$. The measured data is the vector G having the dimension $1 \times M$. The smoothing parameter α is used to regulate the inversion. A solution to this problem is described by Butler et al. [12]. Additional recommended literature is Venkataramanan et al. [13]. We have adapted this method and incorporated a bundle of triangular tubes model in the solution in order to describe the effects of two phases in a porous media. For standard inversion of NMR data the inversion matrix \mathbf{K}_2 will be of the form

$$\mathbf{K}_2 = \begin{bmatrix} \exp(-t_1/T_{2,1}) & \cdots & \exp(-t_1/T_{2,M}) \\ \vdots & \ddots & \vdots \\ \exp(-t_N/T_{2,1}) & \cdots & \exp(-t_N/T_{2,M}) \end{bmatrix}. \quad (3)$$

Incorporating a bundle of triangular tubes model gives a different inversion matrix

$$\mathbf{K} = \begin{bmatrix} m_1(-t_1) & \cdots & m_M(-t_1) \\ \vdots & \ddots & \vdots \\ m_1(-t_N) & \cdots & m_M(-t_N) \end{bmatrix}, \quad (4)$$

where $m_i(t_j)$ is the magnetic signal from the triangular pores i with side length a_i at time t_j . The magnetic signal $m_i(t_j)$ has been found by performing random walk simulations of magnetic decay for two phases simultaneously present in a triangular pore. The decay curves for each phase were fitted to a bi exponential sum given by

$$m_{\text{ph}}(t) = I_{0,\text{ph}} \exp\left(-\frac{t}{T_{0,\text{ph}}}\right) + I_{1,\text{ph}} \exp\left(-\frac{t}{T_{1,\text{ph}}}\right), \quad \text{ph} = o, w. \quad (5)$$

Based on the results from the simulations a correlation for the NMR signal during primary drainage was developed, Lad et al. [10], that gives the intensities I_{0w} , I_{1w} , I_{0o} , I_{1o}

and relaxation times¹ T_{0w} , T_{0o} , T_{1w} , T_{1o} , as functions of surface relaxivity ρ_w , ρ_o , diffusion coefficient D_w , D_o , volumes V_w , V_o and surface contact area A_w and A_o . Volumes V_w , V_o and V_a and areas A_w and A_o are functions of pore size, here given by pore side length a_i , contact angle θ , surface tension σ and capillary pressure P_c . Details for calculating volumes and areas can be found in Helland and Skjaeveland [8]. For fully water saturated pores, we use a correlation based on the results for the NMR signal for one phase in a triangular pore in Hiorth et al. [14]. This correlation will be published in the near future. Adding the bulk relaxation decay and weighting the contribution from each phase by the relative volume gives the magnetic decay for each pore size as

$$m_i(t_j) = \left[\frac{V_w}{V_p} \exp\left(-\frac{t}{T_{2Bw}}\right) \left(\left(I_{0w} \exp\left(-\frac{t}{T_{0w}}\right) \right) + \left(I_{1w} \exp\left(-\frac{t}{T_{1w}}\right) \right) \right) \right]_i \quad (6)$$

$$+ \left[\frac{V_o}{V_p} \exp\left(-\frac{t}{T_{2Bo}}\right) \left(\left(I_{0o} \exp\left(-\frac{t}{T_{0o}}\right) \right) + \left(I_{1o} \exp\left(-\frac{t}{T_{1o}}\right) \right) \right) \right]_i$$

Inverting the signal with this matrix, yields a distribution of pores having side lengths a_i . The reason for using a pore volume of 1 in the inversion is to ensure that all pore sizes are given equal weight in the inversion routine. The bulk relaxation rates for water and oil are annotated as T_{2Bw} , T_{2Bo} .

Wettability index

In this work we use a wettability index, I_{NMR} that is based on the areas of wetted surfaces. The distribution and surface contact areas for each pore are obtained from the inversion routine. This then gives total wetted pore areas for water, $A_{w,Tot}$ and oil $A_{o,Tot}$ in addition to the total pore surface area A_{Tot} , and the wettability index I_{NMR} is given by

$$I_{\text{NMR}} = I_w - I_o = \frac{A_{w,Tot}}{A_{Tot}} - \frac{A_{o,Tot}}{A_{Tot}}. \quad (7)$$

This index has a range of [-1:1], where -1 denotes a fully oil wet system, 0 is neutrally wet and 1 is fully water wet. The wettability index I_{NMR} ignores the effect of the increased contact between oil and pore surface during aging. As the wettability becomes less water wet, the surface affinity for the oil increases and so does the oil surface relaxivity ρ_o , which then in turn can be used in estimating the wettability, Chen et al. [15].

It has been reported that the wettability index can be compared to the spontaneous imbibition measurements, Ma et al. [16]. In this work we use a measure of wettability given by

$$R_{\text{sp.imb}} = \frac{V_{o,\text{sp.imb}}}{V_{o,\text{ini}}} \left(\frac{V_{o,\text{ini}}}{V_{o,\text{sp.imb}}}_{SWW} \right), \quad (8)$$

¹ Relaxation times T_{1w} and T_{1o} should not be confused with longitudinal relaxation time T_1 .

where $V_{o,sp,imb}$ is the volume of produced oil during spontaneous imbibition and $V_{o,ini}$ is the volume of oil originally in place and SWW is under strongly water wet condition. This measure of wettability is based on displaced volumes and can only give a rough estimate of the wettability. We expect that the comparison of $R_{sp,imb}$ with I_{NMR} and I_p will show similar trends but not an $x = y$ match.

EXPERIMENTAL

The data used in this work has previously been published by Siqveland and Skjaeveland [17]. The experiments were initially performed as a method for determining appropriate aging time for cores and therefore some key parameters such as bulk relaxation times are missing and have to be approximated. We have chosen to focus on the CPMG measurements from cores 1, 2, 4, 6 and 8. These cores have kept their names so they can easily be identified in the previous publication, where details of the experimental setup can be found. Berea cores were saturated with synthetic formation water and cores 1, 2, 4 and 6 were flooded with dead crude and left for aging at 90°C for given time intervals. Spectra for T_2 were measured by a CPMG pulse sequence at 35°C by a Resonance Instrument MARAN 2 spectrometer operating at 2 MHz. Spectra were recorded just before and after primary drainage and after aging. Spontaneous imbibition for the cores was measured in Amott cells. Core 8 was flooded with a mixture of two synthetic mineral oils and spontaneous imbibition was measured to benchmark a completely water-wet system.

The NMR data was inverted using our inversion routine based on the method of Butler et al. [10]. The NMR data was first pruned and smoothed by taking an average of 10 points, thus reducing the number of data points from 6144 to 614. Finally the data was adjusted for any potential offset by subtracting the average of the last 10 values in the reduced set of data. The data was then fitted using a bin of 100 logarithmically spaced pore sizes or T_2 values and a smoothing factor α of 0.02.

DESCRIPTION OF METHOD

The T_2 distribution can be used to approximate a pore size distribution. This approximation is based on the fact that in most cases the relaxation time T_2 is proportional to the pore size by a geometric factor and the surface relaxivity. This pore size distribution can then be used to make wettability predictions by adding a pore model for the fluid distributions such as in Looyestijn and Hofman [5]. Our method is somewhat similar in that we use the NMR measurement at 100 % water saturation to find a pore size distribution. The novelty of our method is that we invert NMR data to a distribution of triangular pores. The inversion yields a pore size distribution, and by tuning the parameters of the inversion matrix, we try to match the pore size distribution after flooding to that found at 100 % water saturation. The parameters and fluid distributions can then be used to calculate a wettability index based on wetted areas. The inversion matrix in Eq. 4 is governed by 11 parameters,

$$m_i(t_j) = m_i(\rho_w, \rho_o, D_w, D_o, T_{2Bw}, T_{2Bo}, \theta, P_c, \sigma, a_i, t_j). \quad (9)$$

The pore sizes are given as an array of logarithmically distributed side lengths a_i and the time t_j is given by the NMR measurements. The remaining parameters must then be adjusted to obtain the correct pore size distribution. The capillary pressure P_c and the

surface tension σ are combined in the radius of curvature $r_c = \sigma/P_c$ and this radius is used to tune the inversion result to give the right saturation. Notice the inclusion of diffusion coefficients D_w and D_o in Eq. 9. When the sample is in the Fast Diffusion Limit where the pore size is proportional to the relaxation time, the diffusion coefficient has no or little impact on the inversion and the relaxation of the fluid in each pore is given by a single relaxation time T_2 . However if the pore and the surface relaxivity are sufficiently large, the relaxation is no longer mono exponential and is also a function of the diffusion coefficient. This effect is included in our pore model.

The bulk relaxation T_{2B} of the fluids and the surface relaxivity ρ of the cores were unknown and needed to be estimated. Chen and Song [18] reported a typical pore size for Berea with permeability of 200 mD and porosity of 20 % to be approximately 85 μm . The Berea sandstone used in this work has similar values and so we inverted the average of the NMR data from the 100 % water saturated cores and adjusted the T_{2Bw} and ρ_w until the third peak of the pore size distribution was at 85 μm . The second peak was then located at 15 μm which Chen and Song found to be pore throats. The procedure was repeated for the NMR data from the cores that were flooded with oil, but not aged for the values of the T_{2Bo} and ρ_o until the pore size distribution for the flooded cores resembled that of the cores at 100 % water saturation. Obviously the target pore size can be achieved with different combinations of bulk relaxation and surface relaxivity and we decided on 3 combinations of T_{2B} and ρ given in Table 1, keeping in mind that the bulk relaxation for water is around 1-3 s, T_{2Bo} is lower than T_{2Bw} and ρ_o is equal to or less than ρ_w . The contact angle θ was set to 0 before and after aging as they seemed to have little impact on the wettability index. The diffusion coefficients were set at $D_w = 3 \cdot 10^{-9} \text{ m}^2/\text{s}$ and $D_o = 3 \cdot 10^{-10} \text{ m}^2/\text{s}$.

The inversion matrix is based on bi-exponential decay functions for each phase in the pore as seen in Eq. 6. The individual relaxation times in the bi-exponential functions can be converted to regular relaxation times T_2 and the distribution can be found by sorting the pore size distribution according to relaxation time and weighted by the corresponding intensity.

RESULTS

In Figure 1 we have plotted the pore size distribution from the inversion and the T_2 distribution for core 4 at 100 % water saturation. We see that the distributions are very similar, only differing a small amount at larger pore sizes. From this we can conclude that the core is predominantly in the Fast Diffusion Limit and we need not worry too much about the diffusion coefficients in this case. Still we will be examining the effect of the diffusion coefficient on the pore size distribution from the inversion too see what impact it might have.

In Figure 2-5 the effects of T_{2Bo} , ρ_o , D_o and θ are seen for core 1 after flooding. The distribution consists of 3 peaks located at pore sizes $\sim 10^{-7} \text{ m}$, 10^{-6} m and 10^{-5} m . The first peak represents water filled pores, the second peak consists of water filled pores and pores that have been invaded by oil. The threshold pore size for oil invasion can be seen as the irregularity in the second peak. The third peak is pores invaded by oil. It can be seen that T_{2Bo} mainly affects the distribution of the larger pore sizes. For low values of T_{2Bo} the distribution of the larger pore sizes is spread out and shifted towards larger

pore sizes. For high values of T_{2Bo} the peak is sharp and shifted towards lower values. The relaxivity ρ_o is affecting the middle and the larger pore sizes. Higher values of ρ_o lower the middle peak, heighten the peak of larger pores and shift the peaks towards higher pore sizes. The diffusion coefficient D_o shifts the second and third peak towards higher values and reduces the amplitudes. It seems that although the pore size distributions in Figure 4 indicated that the core was in the Fast Diffusion Limit, variations in D_o still have an impact. The contact angle θ mainly affects the second peak by shifting it towards higher values and reducing the amplitude.

In Figure 6 and Figure 7 we see the pore size distributions for cores 2 and 4 obtained using the Fit 2 parameters in Table 1. We used the same values for ρ_o and T_{2Bo} before and after aging. The pore size distribution for core 2 is quite similar for the core at 100 % water saturation, after flooding and after aging. The pore size distribution for core 4 after aging has a similar shape as the distributions at 100 % water saturation and after flooding, but has moved towards lower pore sizes. This is probably caused by the effects of the wettability change. Core 2 showed little change in wettability in the imbibition test while core 4 had larger change. This change in wettability would change ρ_o .

In Figure 8 we show the distributions of the separate relaxation times for oil and water for core 1 after aging. We compare them to the T_2 distribution obtained by the standard inversion routine. We get a combined distribution that has the same features as the standard T_2 distribution. The new distribution is not so smooth and regular and this is to some extent caused by the sorting algorithm for the new distribution. The second peak is divided into two parts; this is most probably due to a leap in relaxation times, when transcending from water filled to invaded pores. Finally we see a very large water peak at the end of the first peak. This large peak is given by a single T_2 value that represents the water in the invaded pores. The single value is an inherent part of the triangular pore model, where the invaded pores all have the same amount of water present in the corners irrespective of pore size.

Using the values for T_{2B} and ρ from Fit 1, 2 and 3 in Table 1 we calculated wettability indices I_{NMR} before and after aging. We found a fair agreement between the water saturation and the wettability index before aging as seen in Figure 9 and the change in wettability index was positive for all cores as seen in Figure 10, but the trend of the change did not correlate with spontaneous imbibition. We used $R_{sp,imb}$ from Eq. 8 as an indicator of the wettability from the spontaneous imbibition measurements. We found a fair correlation between spontaneous imbibition and wettability index after aging as seen in Figure 11. The wettability index I_{NMR} was in a range of 0.71 and 0.85. Core 8 was used as 100 % water wetted reference in the spontaneous imbibition measurements. It was not measured by NMR and the wettability index was assumed to be 1 before and after aging. These points are plotted as triangular points in Figure 9-12. It can be seen from the figures that the wettability index is quite robust for the different values of T_{2Bw} and ρ_w .

DISCUSSION

Using a triangular pore model will inherently raise some questions as we do not propose that the porous media consist of triangular pores. One issue is that of diffusion regime and surface. To compensate for the low surface area of a triangle in comparison to an

actual pore, one has to increase the surface relaxivity in order to obtain the correct relaxation rate. This can then lead to the wrongful observation that the pore is no longer in the Fast Diffusion Limit, with mono-exponential magnetic decay and the calculations for the magnetic decay may become wrong. On the other hand, the analytical solutions for surface relaxation that are the basis for the diffusion regime parameter $\gamma = \rho R/D$ are all based on magnetic decay in regular geometries with smooth surfaces, [14], [19]. As a result, the diffusion regime parameter is the same for a smooth pore of a given geometry as that of a rugose pore of approximately same geometry. Clearly the added surface area of the latter pore must drive the magnetic decay further towards the Slow Diffusion Limit and multi-exponential decay, although this issue to the knowledge of the authors has not been addressed. Still we expect that the measurements were in the Fast Diffusion Limit and that we might have overestimated the diffusion regime parameter.

There are certain issues with the inversion routine that need to be dealt with before this method might be used for interpreting NMR data. One problem is caused by the smoothing of the distribution that is inherent in the Tikhonov regularization. A mono exponential decay curve with a given relaxation time will be fitted to a sum of exponential decay curves with relaxation times distributed around the actual relaxation time. In other words one can find relaxation times higher than the bulk relaxation time, although these relaxation times do not exist. This problem is also seen when the inversion is performed using the triangular pore model. The inversion routine fits the NMR data to distributions of pore sizes and generates pore sizes that are larger than the actual pore sizes of the core. This in itself is not a major problem but the triangular pore model does not allow for decay curves that relax at higher relaxation times than the bulk relaxation time. This leads to problems for fluids relaxing at bulk relaxation, since the inversion routine can not balance the distribution around the bulk relaxation time. The impact of this is currently not known to the authors and needs to be investigated further. Another problem arises when fluids are relaxing at or close to bulk relaxation times. These fluids are not affected enough by the pore size for the inversion routine to correctly determine the pore size and typically the pore size distribution “flat lines” for pore sizes larger than a certain pore size. In this work we have dealt with this by increasing the bulk relaxation rate for the non wetting fluid, i.e. the oil to 0.8-0.9 s, when the actual value from the T_2 distributions before aging seems to be around 0.4 s. To compensate for the higher bulk relaxation, we increase the surface relaxivity until the pore size distribution is similar to the distribution found at $S_w = 1$. By changing these parameters one also changes the diffusion regime parameter for each pore and the system will appear to be further towards the Slow Diffusion Regime than it actually is. Exactly how much this impact the wettability index is hard to say and must be tested.

I_{NMR} for core 1 is high after aging. Core 1 was the core with the highest S_w and aged for the longest time. During aging the core was not monitored for potential water production and the wettability index might have been found using too high S_w in the inversion. The wettability index I_{NMR} seems to overestimate the water wetness when compared to the spontaneous imbibition tests. We assume that the ratio of actual surface area to triangular area is independent of pore size. This assumption could be false and is perhaps leading to higher water wetness. The wettability index I_{NMR} is solely based on the geometry of the fluids and ignores the effect of the increased contact between oil and pore surface during aging. As the wettability becomes less water wet, the surface affinity for the oil increases and so does the oil surface relaxivity ρ_o , which then in turn

can be used in estimating the wettability. This has been demonstrated by Chen et al. [15] where the wettability indices for each fluid were weighted by the ratio of their respective surface relaxivities to maximum surface relaxivities at strongly wetted conditions. Unfortunately we do not know the maximum oil surface relaxivity for our system and could therefore not calculate the index proposed by Chen et al. [15]. Assuming that the water in our experiments were at the maximum surface relaxivity at all times, we can conclude that the wetting index for oil would become even less and the total wettability index I_{NMR} would show even higher water wetness with the inclusion of surface relaxivity effects.

For future work we intend to investigate if the application of a magnetic field gradient, [4], [20], could help in alleviating the issues with the inversion routine failing for fluids relaxing at bulk relaxation times. We need to test the method thoroughly and examine if the triangular geometry is too simple. The effect of surface relaxivity should be included in the future. We are currently testing the routine on artificial data from triangular pores and plan on performing further tests on actual cores.

CONCLUSION

We have developed a new inversion routine that fits NMR data directly to a distribution of triangular pores. To the knowledge of the authors, this has not been presented elsewhere. The pore model enables us to estimate a pore size distribution, saturation distribution, separate oil and water distributions and a wettability index. The inversion routine was found to give information on the effects of the NMR parameters. The wettability index was in agreement with the spontaneous imbibition measurements and was found to detect the changes in wettability. An additional feature of the inversion routine is that it can be used on systems that are outside the Fast Diffusion Limit and can be combined with measurements with magnetic field gradients [10].

The T_2 distribution from the new inversion routine had the same features as the standard T_2 distribution and was separated into an oil and water distribution showing a distinct peak for the residual water in the pores that had been invaded by oil.

From this work we conclude that the new inversion routine might be used in the future to estimate the wettability after more testing and solving the problems with fluids relaxing at bulk relaxation times and estimating correct wetted areas.

ACKNOWLEDGEMENTS

The authors acknowledge ConocoPhillips and the Ekofisk Coventurers, including TOTAL, ENI, Hydro, Statoil and Petoro, for financing the work and for the permission to publish this paper from the research center COREC.

REFERENCES

1. Borgia G. C., P. Fantazzini and E. Mesini, "Wettability effects on oil-water-configurations in porous media: A nuclear magnetic resonance relaxation study", *Journal of applied physics*, (1991) **70**, 12, 7623-7625.
2. Howard J.J., "Quantitative estimates of porous media wettability from proton NMR measurements", *MRI*, (1998) **6**, 16, 5.
3. Fleury, M. and F. Deflandre, "Quantitative evaluation of porous media wettability using NMR relaxometry", *MRI*, (2003) **21**, 385-387.
4. Freedman, R., N. Heaton, M. Flaum, G. J. Hirasaki, C. Flaum, and M. D. Hürlimann, "Wettability, saturation, and viscosity using the magnetic resonance fluid characterization method and new diffusion-editing pulse sequences", Paper SPE 77397 presented at the Annual Technical Conference and Exhibition, San Antonio, Texas, 29 September-2 October 2002.
5. Looyestijn, W. and J. Hofman, "Wettability determination by nuclear magnetic resonance", *SPEEE*, (2005) **9**, 2, 146-153. SPE-93624-PA.
6. Øren, P.E., F. Antonsen, H. G. Rueslåtten and S. Bakke, "Numerical simulations of NMR responses for improved interpretations of NMR measurement in reservoir rocks", Paper SPE 77398 presented at the SPE Technical Conference and Exhibition in San Antonio, Texas, 29 September – 2 October 2002.
7. Helland, J. and S. M. Skjæveland, "Three-phase mixed-wet capillary pressure curves from a bundle of triangular tubes model", *Journal of Petroleum Science and Engineering*, 2006a **52**, 100–130.
8. Helland, J. and S. M. Skjæveland, "Physically based capillary pressure correlation for mixed wet reservoir from a bundle of tubes model", *SPEJ*, 2006b **11**, 2, 171-180. SPE-89428-PA.
9. Al-Mahrooqi, S.H., C.A. Grattoni, A.H. Muggerridge, and X.D. Jing, "Pore-scale modelling of NMR relaxation for the characterization of wettability", *Journal of Petroleum Science and Engineering*, (2006) **52**, 1-4, 172-186.
10. Lad, U.H., A. Hiorth, J. Finjord and S. M. Skjæveland, "Two-phase simulation and correlation of NMR magnetic decay in equilateral triangular pores", Poster presented at the International Symposium of the Society of Core Analysts, Abu Dhabi, UAE, 29 October-2 November 2008.
11. Tikhonov, A.N. and V. Y. Arsenin, *Solutions of ill-posed problems*, Wiley, New York, (1977).
12. Butler, J. P., J. A. Reeds and S. V. Dawson, "Estimating solutions of first kind integral equations with nonnegative constraints and optimal smoothing", *SIAM J. Numer. Anal.*, (1981) **18**, 3, 381–397.
13. Venkataramanan, L., Y. Q. Song, and M. D. Hürlimann, "Solving fredholm integrals of the first kind with tensor product structure in 2 and 2.5 dimensions", *IEEE Transactions on signal processing*, (2002) **50**, 5, 1017 - 1026.
14. Hiorth, A., U. H. Lad, J. Finjord and S. M. Skjæveland, "NMR for equilateral triangular geometry under conditions of surface relaxivity-analytical and random walk solution", *Transport in Porous Media*, (2006) **69**, 1, 33-53.
15. Chen, J., G. J. Hirasaki and M. Flaum, "NMR wettability indices: Effect of OBM on wettability and NMR responses", *Journal of Petroleum Science and Engineering*, (2006) **52**, 161-171.
16. Ma, S., N. R. Morrow, X. Zhang, and X. Zhou, "Characterization of wettability from spontaneous imbibition measurements", *JCPT*, (1999) **38**, 13, 1-8

17. Siqveland, O.K. and S. M. Skjaeveland, "Aging time control by NMR relaxation", Paper presented at the 7th International Symposium on Reservoir Wettability, Freycinet, Tasmania, Australia, 12-14 2002.
18. Chen, Q. and Y. Q. Song, "What is the shape of pores in natural rocks?", *Journal of Chemical Physics*, (2002) **116**, 19, 8247-8250.
19. Brownstein, K. and C. Tarr, "Importance of classical diffusion in NMR studies of water in biological cells", *Phys. Rev. A*, (1979) **19**, 2446-2453.
20. Sørland, G. H., H. W. Anthonsen, J. G. Seland, F. Antonsen, H. C. Wideroe, and J.Krane. "Exploring the separate NMR responses from crude oil and water in rock cores", *Applied Magnetic Resonance*, (2004) **26**, 3, 417-425.

TABLES AND FIGURES

Table 1. NMR properties for water and oil.

Water	Fit 1	Fit 2	Fit 3	Unit
T_{2Bw}	1.0	2.0	3.0	[s]
ρ_w	$37 \cdot 10^{-6}$	$45 \cdot 10^{-6}$	$47 \cdot 10^{-6}$	[m/s]
Oil				Unit
T_{2Bo}	0.8	0.9	0.9	[s]
ρ_o	$37 \cdot 10^{-6}$	$45 \cdot 10^{-6}$	$47 \cdot 10^{-6}$	[m/s]

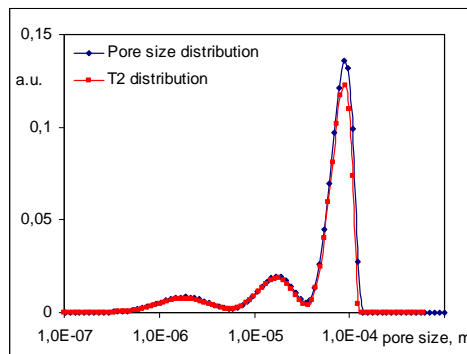


Figure 1. Pore size distribution from inversion routine and T_2 distribution for core 4 at $S_w = 1$.

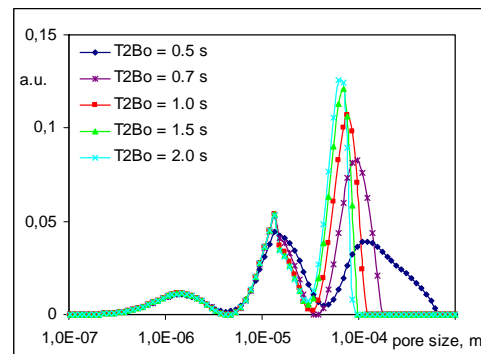


Figure 2. Effect of T_{2Bo} on pore size distribution for core 1 after flooding.

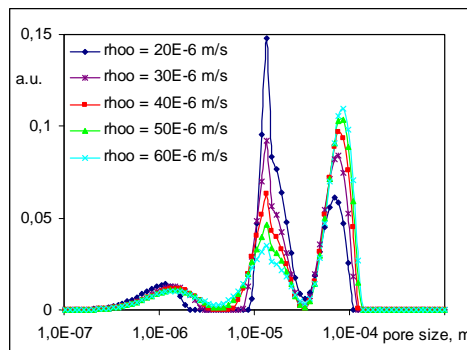


Figure 3. Effect of ρ_o on pore size distribution for core 1 after flooding.

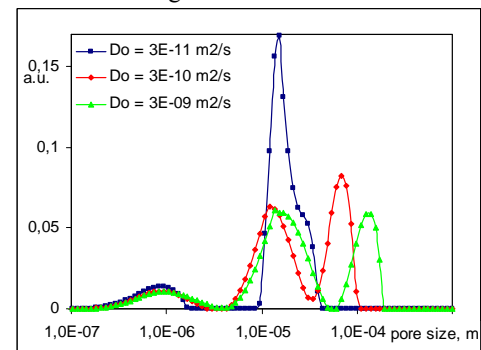


Figure 4. Effect of D_o on pore size distribution for core 1 after flooding.

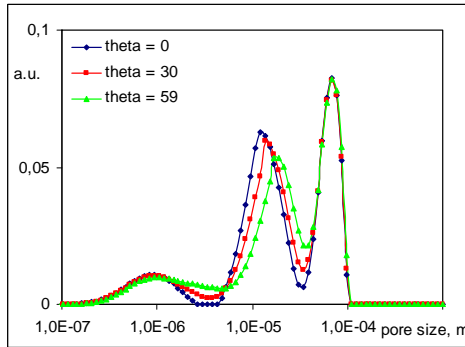


Figure 5. Effect of θ on pore size distribution for core 1 after flooding.

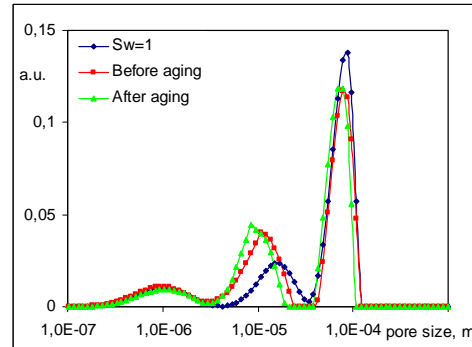


Figure 6. Pore size distribution for core 2 at $S_w = 1$, after flooding and after aging.

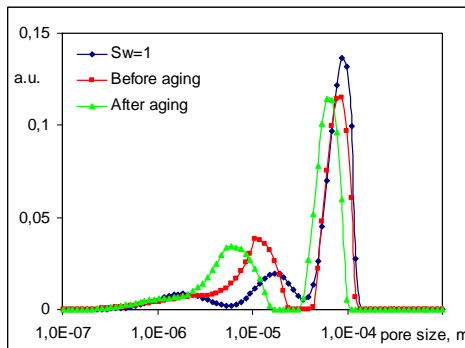


Figure 7. Pore size distribution for core 4 at $S_w = 1$, after flooding and after aging..

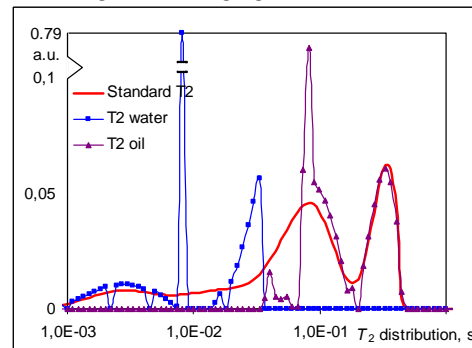


Figure 8. Standard T_2 distribution and inversion T_2 distribution for oil and water for core 1 after aging.

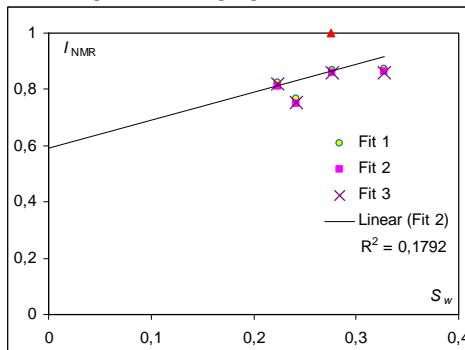


Figure 9. Comparison of wettability index, I_{wo} , before aging and water saturation, S_{wr} .

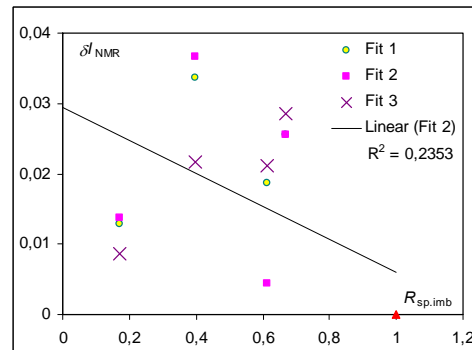


Figure 10. Comparison of change in wettability index, δI_{wo} , and produced oil fraction of oil in place, OIP.

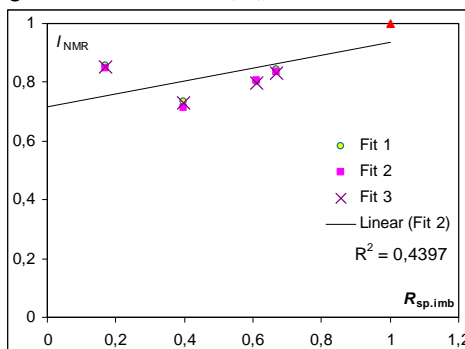


Figure 11. Comparison of wettability index, I_{wo} , after aging and produced oil fraction of oil in place, OIP.